

Deuterated species in the star-forming regions

Magda Kulczak-Jastrzębska¹, Dariusz Lis^{2,3}, Agata Karska⁴ and Maryvonne Gerin²

1. Astronomical Observatory of the Jagiellonian University, Orla 171, 30-244 Kraków, Poland; kulczak@oa.uj.edu.pl
2. École Normale Supérieure, CNRS, Observatoire de Paris, UMR 8112, LERMA, Paris, France
3. Caltech, Cahill Center for Astronomy and Astrophysics, 301-17, Pasadena, CA 91125, USA
4. Astronomical Observatory of the Adam Mickiewicz University, Słoneczna 36 60-286 Poznań, Poland

High deuteration levels in isolated prestellar cores can be explained by gas-phase or grain surface chemistry in dense, cold regions where abundant gas-phase species are frozen onto dust grains. We argue that an alternative mechanism may operate in dense gas in the vicinity of embedded young stellar objects, where slow C-type shocks associated with molecular outflows may produce conditions favorable for deuterium fractionation.

1 Introduction

High deuteration levels in isolated prestellar cores can be explained by gas-phase or grain surface chemistry in dense, cold regions where abundant gas-phase species are frozen onto dust grains. An alternative mechanism, slow C-type shocks associated with molecular outflows, may produce conditions for deuterium fractionation reactions by (i) increasing the gas volume density and thus shortening the depletion and gas-phase reaction time-scales or (ii) sputtering/injecting the grains mantles because of the passage of a shock. $\text{DCO}^+(3-2)$ emission traced the spatial distribution of deuterated molecules is often displaced with respect to the highest column density region traced by submillimeter dust emission and sometimes associated with the high-velocity outflow activity.

2 Observations

Spectroscopic observations presented here were carried out in 2002-2007 using the 230 GHz facility receiver and spectrometers of Caltech Submillimeter Observatory (CSO) on Mauna, Kea Hawaii, as backups to various high-frequency programs. The CSO beam size at 230 GHz is $\sim 30''$ and the main beam efficiency is $\sim 60\%$. The 350 μm continuum observations were carried out in 2003 using the SHARC II bolometer camera.

3 Preliminary results

Barnard 1: DCO^+ is spatially displaced with respect to the continuum emission and clearly located in the vicinity of apex of $\text{CO}(2-1)$ outflows. The main DCO^+

peak is associated with B1-b continuum source (ND₃ detected - Lis et al. (2002)), secondary peak is associated with B1-c. The red lobe of the outflow centered in B1-c encompasses the DCO⁺ peak associated with B1-b. **NGC 1333**: A bright DCO⁺ ridge is located NE of IRAS 4A (ND₃ detected -van der Tak et al. (2002)). Secondary DCO⁺ peak corresponds to 51 (SK16)-starless core. The morphology of this region is similar to that in L1157-B1 chemically rich shocked region where dust is not heated by protostar. The secondary DCO⁺ peak is located on-axis of the famous molecular outflow associated with the HH 7-11 sources, centered SSV13 and the DCO⁺ source is again encompassed by the blue-shifted outflow lobe. Relatively weak ND₃ emission has also been detected at this location Roueff et al. (2005). **LDN 1641**: The DCO⁺ peak near VLA 3 is located to the west of the red lobe of the VLA 3 outflow, near the edge of the redshifted high-velocity emission.

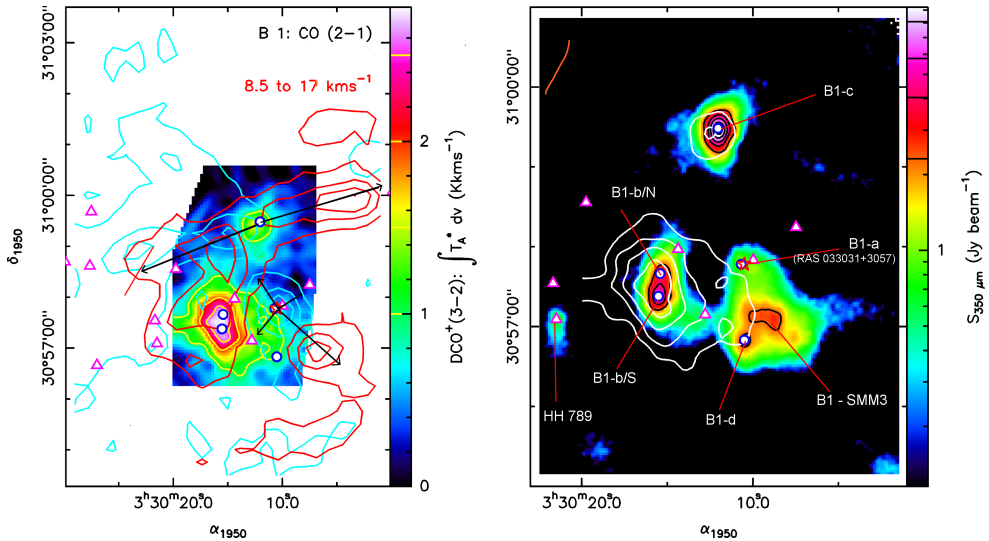


Fig. 1: (*Left*) Distribution of DCO⁺(3 – 2) emission in Barnard 1 (color image and yellow contours) with overlaid contours of high-velocity CO(2 – 1) emission (blue and red contours respectively, dark arrows mark jets). (*Right*) Distribution of the 350 μm dust continuum emission (color image and black contours) with overlaid white contours of DCO⁺(3 – 2) emission. Red stars marks the location of IRAS 03301+3057. Magneta triangles mark locations of HH objects (Walawender et al., 2005) and blue circle mark compact continuum source B1-a to d (Hatchell et al., 2005).

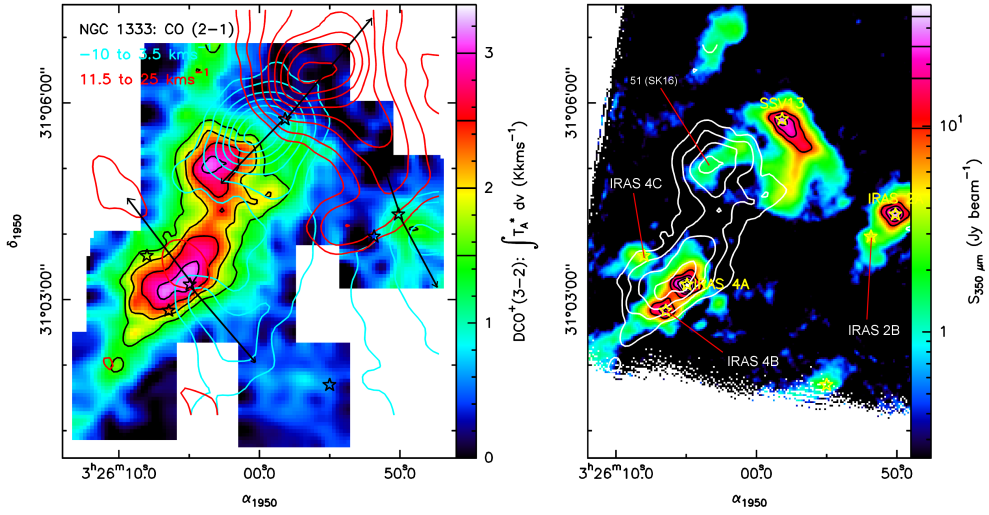


Fig. 2: (Left) Distribution of $\text{DCO}^+(3-2)$ emission (color image and black contours) with overlaid contours of high-velocity $\text{CO}(2-1)$ emission (blue and red contours respectively, dark arrows mark jets). (Right) Distribution of the $350 \mu\text{m}$ dust continuum emission (color image and black contours) with overlaid white contours of $\text{DCO}^+(3-2)$ emission.

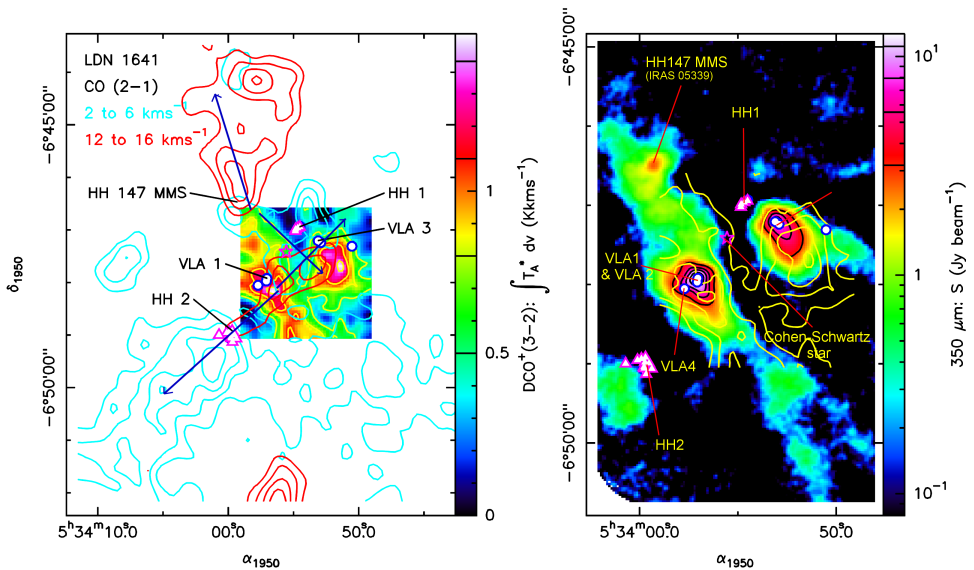


Fig. 3: (Left) Distribution of $\text{DCO}^+(3-2)$ emission (color image and yellow contours) with overlaid contours of high-velocity $\text{CO}(2-1)$ emission (blue and red contours respectively, dark arrows mark jets). (Right) Distribution of the $350 \mu\text{m}$ dust continuum emission (color image and black contours) with overlaid yellow contours of $\text{DCO}^+(3-2)$ emission.

References

- Hatchell, J., Richer, J. S., Fuller, G. A., et al., *Star formation in Perseus. Clusters, filaments and the conditions for star formation*, A&A **440**, 151 (2005)
- Lis, D. C., Roueff, E., Gerin, M., et al., *Detection of Triply Deuterated Ammonia in the Barnard 1 Cloud*, ApJ **571**, 332 (2002)
- Roueff, E., Lis, D. C., van der Tak, F. F. S., et al., *Detection of Triply Deuterated Ammonia in the Barnard 1 Cloud*, A&A **438**, 585 (2005)
- van der Tak, F. F. S., Schilke, P., Miller, H. S. P., et al., *Triply deuterated ammonia in NGC 1333*, A&A **388**, L53 (2002)
- Walawender, J., Bally, J., Kirk, H., Johnstone, D., *Multiple Outflows and Protostars in Barnard 1*, AJ **130**, 1795 (2005)